Engineering dynamical entanglement of a conditionally kicked membrane in cavity optomechanics

Usman Ali[1], Sara Medhet[2], Abid Ali[1], and Farhan Saif[2*]

[1]*Department of Physics, Quaid-i-Azam University, Islamabad 45320, Pakistan;*
[2]*Department of Electronics, Quaid-i-Azam University, Islamabad 45320, Pakistan*

In optomechanical configuration we show the entanglement of a suspended nano-mechanical membrane with optical driving field. In the presence of an optical field, the high finesse optomechanical resonator acts as an oscillator driven by a radiation pressure force. The periodic radiation pressure force acting on the nano-mechanical membrane in the optomechanical system is considered as a kicked harmonic oscillator. We explain entanglement based upon the system parameters employing conditionally kicked scenario. It is shown that the present-day experimental advancement allows an appropriate control of parameters, namely the frequency ratio, the kicking strength and specially the Lamb-Dicke parameter. We found that the dynamics strictly follow correspondence principle in the semi-classical limit which was not the case in previous work [34].

chaotic system, quantum chaos, driven system, kicked harmonic oscillator, quantum entanglement, nonseperable states, floquet states, optomechanics, optomechanical entanglement.

1 Intriduction

Optomechanical systems have recently got significant interest as a promising architecture which provides a platform for realizing quantum mechanical effects. The field of optomechanics has witnessed considerable breakthroughs, including entangling states of resonator [1-3], quantum superposition states [4, 5], ground-state cooling[6] and so on. With the advent of quantum information[7], the protagonist of entanglement in chaotic systems has been highlighted[8-11]. Though the entanglement can be observed in many systems without chaos but the plus point of using quantum chaotic system is its faster rate of achievement. The pursuit of quantum chaos has led to the realization of kicked Hamiltonian which are well-suited model for studying chaos. A lot of work has been done in this regard examining models like kicked rotator and kicked harmonic oscillator (KHO). Even though, kicked rotator models are intensely discussed for their viability to Kolmogorov-Arnold-Moser (KAM) theorem, the quest of KHO with non-KAM behavior is still outstanding. KHO has received enormous attention because of its captivating dynamical properties and is theoretically modelled in large number of varying systems, like one studying quantum transport in superlattices[12] and the other for Bose-Einstein Condensate in presence of a parabolic confining trap[13], suggested in Paul ion traps[14] , could also be done by manipulating ultracold atoms in optical lattices[15]. Recently, some experimental work related to realization of KHO has appeared which may lead to further investigations of quantum nonlinear dynamics[16].

Quantum chaotic system holds an elusive property of entanglement. Studies have shown that entanglement increases

as the chaotic parameter is enhanced[8, 17]. Also, in some systems the increase in chaos may lead to the saturation of entanglement generation[18]. Cavity optomechanics provides a versatile platform to study entangled states. Exploring interaction between electromagnetics and mechanical modes[19, 20]. It gives an alternative view of entangling two mechanical oscillators such as optomechanical interferometer[21, 22], optomechanical radiation pressure[23-27], optomechanical interfaces having quantum interference[28]. In our study we mainly focused on Delta kicked harmonic oscillator in cavity optomechanics which has been engineered considering nano-mechanical membrane inside the cavity. Classical dynamics of this mechanical oscillator are well described and found to have phase space of stochastic webs leading to complete chaotic dynamics[29]. In [30] the authors suggest that in such an experimental scenario the membrane can be cooled to its ground state. Also, as the motion of mechanical membrane is governed by field inside the cavity so one escaping photon from the cavity takes the oscillator to a single phonon Fock state [33]. We study the photon-phonon Entanglement, sprouting with each δ-pulse of the driving field. Quantum state after a kick to immediately after the next kick is controlled by the Floquet operator. In Ref. [34] authors explore the Floquet operator's ability to create entanglement in KHO and show how entanglement grows with time. In this paper we present experimental suggestions which would be realizable for a proper parametric control. Moreover, semi-classical limit, $\hbar_{eff} \to 0$, is being explored, showing how entanglement, a purely quantum phenomenon with no classical analogue, behaves in such a limit.

The paper is organized as follows: In Sec. (2), we present the experimental model of the system. We introduce the entanglement measures in Sec. (3). Numerically observed entanglement dynamics, dictated by system parameters, are described in Sec. (4). Finally, Sec. (5) summarise the findings.

2 Model

We consider a double-cavity optomechanical system, illustrated in Fig. (1), with perfectly reflecting nano-mechanical membrane that receives the radiation pressure from both the cavity A & B. Two controllable laser beams, with frequencies ν_A and ν_B, drive the cavities with reference to fixed transmissive mirrors at both ends, with amplitudes ζ_A and

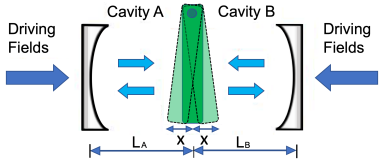

Figure 1 Schematic illustration of the optomechanical configuration: A perfectly reflecting nano-mechanical membrane receives radiation pressure from both ends through two transmissive fixed cavity mirrors.

ζ_B, respectively. In the interaction picture the Hamiltonian $H = H_o + H_c$ thus consists of two parts,

$$H_0 = \frac{p^2}{2m} + \frac{1}{2}m\omega^2 x^2, \tag{1}$$

$$H_c = \hbar(\omega_A - G_A x)a^\dagger a + \hbar(\omega_B + G_B x)b^\dagger b + \hbar(\zeta_A e^{-i\nu_A t}a + \zeta_B e^{i\nu_B t}b + H.C.). \tag{2}$$

Here, H_o accounts for the free Hamiltonian of the mechanical membrane, whereas m is the effective mass of resonating membrane with frequency ω. The Hamiltonian H_c describes optical fields and their coupling to mechanical membrane, that is, $G_A = \omega_A/L_A$ and $G_B = \omega_B/L_B$, with L_A & L_B being the fixed cavity lengths, as in [35]. We consider that both the cavities have symmetric setup, i.e. $\omega_A = \omega_B$, $\nu_A = \nu_B = \nu$, $\zeta_A = \zeta_B = \zeta$, $\Delta_A = \Delta_B = \Delta$, $L_A = L_B = L$, and $G_A = G_B = G$. Under this consideration, periodic switching of the controllable laser driving field and working in the regime of short time of interaction between cavity field and membrane, the mechanical membrane becomes kicked harmonic oscillator. Moreover, working with a driving field of fixed amplitude $\zeta = \zeta_0$, in which the perturbation consists of consecutive δ-pulses, makes the nano-mechanical membrane as Delta Kicked Harmonic Oscillator, specifically with a hyperbolic potential [29]. The effective Hamiltonian of the system is approximated to be,

$$H_{eff} = \frac{p^2}{2m} + \frac{1}{2}m\omega^2 x^2 - k\cosh\alpha x \sum_{n=-\infty}^{n=\infty}\delta(t - nT), \tag{3}$$

where, $k = 2\hbar\zeta_0/\Delta$ is the kick strength and $\alpha = \sqrt{2}\omega_A/L\Delta$. We redefine the system in terms of a two-level system, and after a suitable scaling

$$H' = \frac{1}{2}(X^2 + P^2) - K[\cosh(X)]|0_z\rangle\langle 0_z| \sum_{n=-\infty}^{n=\infty}\delta(t - nT), \tag{4}$$

with $X = \alpha x$; $P = p\alpha/m\omega$. Moreover, $K = (k\alpha^2)/m\omega$ is the renormalized kicking strength, and $\tau = \omega t$ is the

scaled time, which introduces dimensionless frequency ratios (kick to kick period), i.e. q, redefining time as $\tau = 2\pi/q$. Yong Li et al. [30], proposes a scheme to cool down mechanical resonator to its quantum ground state. Starting with the resonator in ground state $|0_z\rangle$, the outer product $|0_z\rangle\langle 0_z|$ is introduced. Now, both cavities pumped by external laser pulse within blue detuned regime, the resonator is excited to a single phonon folk state $|1_z\rangle$ [31-33]. For a short time mirror field interaction, a superposition state $|\Psi_c\rangle = \frac{1}{\sqrt{2}}(|1_A\rangle|0_B\rangle + |0_A\rangle|1_B\rangle)$ is prepared in both cavities (A) and (B). The consecutive kick provides the radiation pressure force and in this way the intracavity photon state evolves together with mechanical resonator.

The non-classical dynamics of kicked membrane is governed by Floquet operator which determines the dynamics between two consecutive kicks such that the state just before a kick is mapped on the state before the previous kick. The conditionally kicked membrane evolves in time by the conditional Floquet operator. For this, we assume that driving laser fields are far-detuned and the membrane is cooled to its ground state. Now for most of the time the membrane will remain in the no phonon state and the excited state is in adiabatic approximation. Hence, we can say that in the limit of large detuning the membrane is conditionally kicked with kick part only addressing the ground state wave function. For computational convenience, we write the conditional Floquet operator as,

$$\hat{F} = e^{-i(\hat{a}^\dagger a + \frac{1}{2})\tau} e^{i\frac{K}{\hbar_{eff}}\cosh\left[\sqrt{\frac{\hbar_{eff}}{2}}(\hat{a}+\hat{a}^\dagger)\right]|0_z\rangle\langle 0_z|} = \hat{U}_0\hat{U}_k, \tag{5}$$

where, $\hat{U}_0$ represents the harmonic oscillator free evolution between the kicks and $\hat{U}_k$ is the Kick evolution operator. We have introduced the effective Planck's constant, $\hbar_{eff} = \frac{\hbar\omega^2}{m\omega}$. Keeping $\Delta/2\pi = 10^7$Hz, m = 50Pg, L = 5μm, $\omega/2\pi$ = 134KHz and $\omega_A/2\pi = 7 \times 10^{14}$Hz, we obtain $\hbar_{eff} = 1$. Also the value of kicking strength K = 0.01 is fixed by adjusting controllable driving field amplitude ζ_o to the order 10^6Hz, which does not exceed the maximum threshold of cooling [29]. Now, Floquet operator has three parameters: K, τ and η. This contrasts with the classical evolution which depends only on the first two parameters. No change of variables is going to remove the dependence on η. We sequently discuss different responses to the entanglement based on these parameters.

3 Entropy of Entanglement

Von Neumann entropy is a preferred measure of entanglement for bipartite quantum states, which is given by corresponding reduce density operators of the quantum system (Y and Z) [36, 37]. For a pure state it is defined as:

$$E(\rho) = S(\rho_y) = S(\rho_z), \tag{6}$$

Where, $S(\rho)$ is the von Neumann Entropy of one of the reduced density matrix given by,

$$S = tr(\rho ln\rho) = -\langle ln\rho\rangle, \tag{7}$$

To investigate entanglement dynamics of the conditionally delta-kicked membrane, we use linear entropy. Von Neumann entropy, the actual description of entanglement, approximates to the linear entropy which mainly simplifies the usual relation,

$$S = 1 - tr(\rho^2). \tag{8}$$

Linear entropy is a lower order approximation to the von Neumann entropy expanded in formal Mercator series of the logarithm retaining just the leading term [38, 39]. Linear entropy satisfies all the physical requirements of a measure of quantum correlations and is a similar measure of the degree of mixing of the state to the von Neumann Entropy. However, it is much easier to calculate and also obviates us from the cumbersome diagonalization of reduced density operators.

Now, starting with the initial state given by the ancilla,

$$|\psi_{YZ}(0)\rangle = \frac{|\phi_y\rangle|0_z\rangle + |\vartheta_y\rangle|1_z\rangle}{\sqrt{2}}, \tag{9}$$

$|\phi_y\rangle, |\vartheta_y\rangle$ are the states of the field inside each cavity and $|0_z\rangle, |1_z\rangle$ are the phonon Fock states. Both mirror states, living in superposition, correlates to the field states. The entangled state prepared evolves in time following the Floquet Dynamics. From the usual definition of conditional Floquet Operator, we know that the deriving only contribute to ground state phononic mode. So, after n kicks the result will be an entangled state of the form,

$$\begin{aligned}|\psi_{YZ}(Nt)\rangle =& \hat{F}^N|\psi_{YZ}(0)\rangle,\\ =& \frac{\hat{F}^N|\phi_y\rangle|0_z\rangle + \hat{F}^N|\vartheta_y\rangle|1_z\rangle}{\sqrt{2}},\\ =& \frac{\hat{F}^N|\phi_y\rangle|0_z\rangle + \hat{U}_0^N|\vartheta_y\rangle|1_z\rangle}{\sqrt{2}}.\end{aligned} \tag{10}$$

The corresponding Density Matrix of the combined system will be,

$$\begin{aligned}\hat{\rho}_{YZ} =& \ |\psi_{YZ}(Nt)\rangle\langle\psi_{YZ}(Nt)|,\\ =& \frac{1}{2}\Big[(\hat{F}^N|\phi_y\rangle|0_z\rangle + \hat{U}_0^N|\vartheta_y\rangle|1_z\rangle)(\hat{F}^N|\phi_y\rangle|0_z\rangle + \hat{U}_0^N|\vartheta_y\rangle|1_z\rangle)^\dagger\Big],\\ =& \frac{1}{2}\Big[\hat{U}_0^N|\vartheta_y\rangle|1_z\rangle\langle 1_z|\langle\vartheta_y|\hat{U}_0^{N^\dagger} + \hat{F}^N|\phi_y\rangle|0_z\rangle\langle 0_z|\langle\phi_y|F^{N^\dagger}\end{aligned}$$

$$+\hat{F}^{N}|\phi_{Y}\rangle|0_{Z}\rangle\langle 1_{Z}|\langle\vartheta_{Y}|\hat{U}_{0}^{N\dagger}+\hat{U}_{0}^{N}|\vartheta_{Y}\rangle|1_{Z}\rangle\langle 0_{Z}|\langle\phi_{Y}|\hat{F}^{N\dagger}\Big]. \tag{11}$$

Using the property of Tensor Products, i.e. $(a\otimes b)(c\otimes d) = ac\otimes bd$, we get the final simplified form of density matrix

$$\hat{\rho}_{YZ}=\frac{1}{2}\Big[|1_{Z}\rangle\langle 1_{Z}|\hat{U}_{0}^{N}|\vartheta_{Y}\rangle\langle\vartheta_{Y}|\hat{U}_{0}^{N\dagger}+|0_{Z}\rangle\langle 0_{Z}|\hat{F}^{N}|\vartheta_{Y}\rangle\langle\vartheta_{Y}|\hat{F}^{N\dagger}$$
$$+|0_{Z}\rangle\langle 1_{Z}|\hat{F}^{N}|\phi_{Y}\rangle\langle\vartheta_{Y}|\hat{U}_{0}^{N\dagger}+|1_{Z}\rangle\langle 0_{Z}|\hat{U}_{0}^{N}|\vartheta_{Y}\rangle\langle\phi_{Y}|\hat{F}^{N}\Big]. \tag{12}$$

As we know that reduced density matrices of the bipartiate states are given by, $\hat{\rho}_{Y}=tr_{Z}(\hat{\rho}_{YZ})$ and $\hat{\rho}_{Z}=tr_{Y}(\hat{\rho}_{YZ})$. Thus, on solving, we end to

$$\hat{\rho}_{Z}=\frac{1}{2}\Big[\hat{I}+|0_{Z}\rangle\langle 1_{Z}|\langle\vartheta_{Y}|\hat{U}_{0}^{N}\hat{F}^{N}|\phi_{Y}\rangle+|1_{Z}\rangle\langle 0_{Z}|\langle\phi_{Y}|\hat{F}^{N\dagger}\hat{U}_{0}^{N}|\vartheta_{Y}\rangle\Big], \tag{13}$$

also,

$$\hat{\rho}_{Z}^{2}=\frac{1}{2}+\frac{1}{2}|\langle\phi_{Y}|\hat{F}^{N\dagger}\hat{U}_{0}^{N}|\vartheta_{Y}\rangle|^{2}. \tag{14}$$

Entanglement can now easily be calculated through the linear entropy

$$S=2[1-tr(\rho_{Z}^{2})],$$
$$=2[1-\frac{1}{2}-\frac{1}{2}|\langle\phi_{Y}|\hat{F}_{0}^{N\dagger}\hat{U}_{0}^{N}|\vartheta_{Y}\rangle|^{2}]. \tag{15}$$

Here, we used the fact: $\hat{\rho}_{Y}=\hat{\rho}_{Z}$. Thus linear entropy can be calculated through,

$$S=1-|\langle\phi_{Y}|\hat{F}^{N\dagger}\hat{U}_{0}^{N}|\vartheta_{Y}\rangle|^{2}=1-|\langle\phi_{Y}|(\hat{U}_{0}^{\dagger}\hat{U}_{K}\hat{U}_{0})^{N}|\vartheta_{Y}\rangle|^{2}. \tag{16}$$

We do not try to resolve this expression analytically. Although some theoretical work has been done for the Floquet states, using split operator technique [40]. It would be a daunting task to solve this problem using the explicit expressions of Floquet operators, containing infinite summations of Bessel functions, even for few kicks. Instead, we attempt to extract useful information numerically by investigating the behavior of entropy of entanglement.

4 Numerical Results

Initially it is supposed that the field inside each cavity is coherent, $|\vartheta_{Y}\rangle=|\phi_{Y}\rangle=|\beta_{Y}\rangle$, thus at first there is no entanglement. Entanglement is mainly generated by the action of conditional Floquet operator when different ratios τ are considered. Entanglement versus number of kicks is being plotted varying τ and some other parameters immanent in the definition of Floquet operator. We have fixed $\eta=1/\sqrt{2}$, $K=0.01$ from Fig. 2 to Fig. 5 and plotted the behavior of entanglement considering different initial states of the field. As the dynamics of kicked membrane differs depending upon the choice of q, being rational or irrational [29]. So, entanglement dynamics are explored for both rational and irrational outcomes of q.

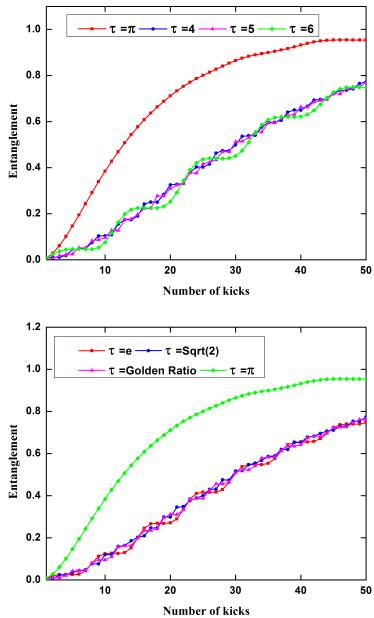

Figure 2 Entanglement versus number of kicks for $K=0.01$ and $\hbar_{eff}=1$ upon varying frequency ratio τ. The initial state was taken as a product of the ancilla and a coherent state with $\beta=2$.

In Fig. 2 (above), entanglement evolution is shown for $\tau=\pi$ and $\tau=\{4,5,6\}$ for a coherent state with $\beta=2$. Note that while entanglement grows rapidly for $\tau=\pi$, approaching unity for few kicks, it increases steadily for the integers $\tau=\{4,5,6\}$. This indicates a rise in entanglement evolution for irrational rates, but this behavior is not consistent i.e. there are some irrationals for which entanglement increases as linearly as those integers, as shown in Fig. 2 (be-

low), for irrational ratios $\tau = \sqrt{2}$, $(\sqrt{5}+1)/2$, e. There is a clear analogy between the trends in Fig. 2, and it is eminent that the ratio $\tau = \pi$ leaps out from the other irrational ratios. Moreover, same trends are being observed whenever $\tau = p\pi, p = 1, 2, 3...$, i.e. fixing the other parameters, all the curves overlap. To further investigate this phenomenon, we consider another initial condition that is the product of ancilla with Fock state. In that case the initial states $|\vartheta_\gamma\rangle = |\phi_\gamma\rangle$ would be equal to $|n_\gamma\rangle$, which is representing the Fock state. Taking a Fock state with number, i.e. $n = 10$, when plotting entanglement evolution in Fig. 3 (above),

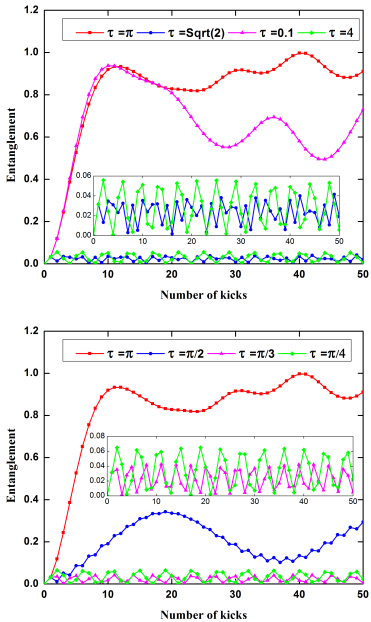

Figure 3 Entanglement versus number of kicks for $K = 0.01$ and $\hbar_{eff} = 1$ upon varying frequency ratio τ. The initial state was taken as a product of the ancilla and fock state with $n = 10$.

keeping the same parametric values as used previously, again the ratio $\tau = \pi$ segregates from the other rates and entanglement oscillates for integer values followed by many death and revivals of entanglement. Like the above discussed case, here exist some multiples of π as well, in fact, $\tau = p\pi$, at which entanglement is enhanced. Interestingly, the numerical simulations with the initial Fock state report a decline in entanglement rate for $p = 1/2$ and a robust collapse for $p = 1/3$ and $1/4$, as can be seen from Fig. 3 (below). We noticed the same behavior for other rational values of p. However, these trends vary quantitatively based on the initial conditions and choice of parametric values, depending upon our numerical experiment with coherent and Fock states if the parameters K, η and h_{eff} are taken to be fixed, qualitatively this behavior remains constant.

Now we examine entanglement, evolving at each kick, when the kicking strength K is varied. For this, we choose the same value of the Lamb-Dicke parameter as before, fixed at $\eta = 1/\sqrt{2}$ and the ratio $\tau = \pi$, which as we came to know optimizes the entanglement. Entanglement versus number of kicks are plotted for the product of ancilla and coherent state, as before. It can be seen in Fig. 4, entanglement diminishes upon reduced kick strengths, while it is enhanced for an increase. In particular, entanglement rises and starts to oscillate rapidly for higher values of K. Keeping in mind that for a delta pulse with large kicking frequency, $\tau = 2\pi\omega/\omega_k \to 0$, entanglement is mainly generated and affected only by the kick term of Eq. (5). Thus one could estimate from the result that if kicking strength is increased, maximum entanglement can be attained even at first kick irrespective of the ratio τ.

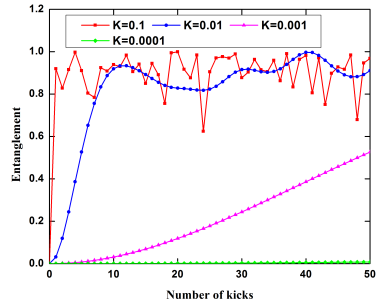

Figure 4 Entanglement versus number of kicks for $\hbar_{eff} = 1$ and $\tau = \pi$ upon varying kick strength K. The initial state was taken as a product of the ancilla and fock state with $n = 10$.

4.1 Semi-Classical Dynamics

Ultimately, we probe the semi-classical limit and analyse how entanglement behaves with $\hbar_{eff} \to 0$. Specifically, in the conditionally kicked membrane setting, varying $\hbar_{eff}$ is straightforward by adjusting the parameter α. As entanglement is a purely quantum entity, short of any classical counterpart, one could predict a vanishing entanglement as $\hbar_{eff}$ reduces to negligible values. To construe this prominent be-

haviour, we have fixed the other two relevant parameters, τ and K, while varying $\hbar_{eff}$. The results obtained are shown in Fig. 5 (above) for three values of $\hbar_{eff}$, which are mainly followed by other similar values of $\hbar_{eff}$. As expected, entanglement increases as the value of $\hbar_{eff}$ is raised and it decreases as soon as $\hbar_{eff}$ is reduced, unless entanglement rate saturates for $\hbar_{eff} < 0.1$.

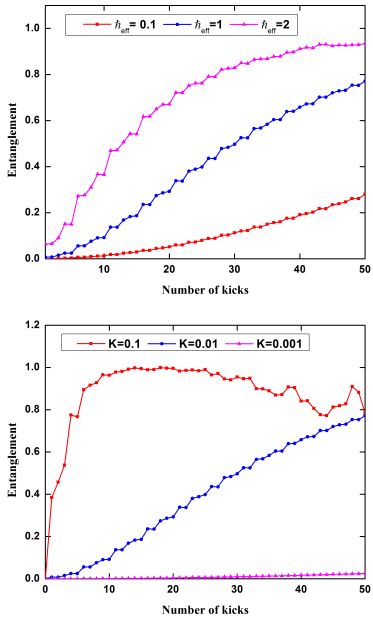

Figure 5 Entanglement versus number of kicks (a) for a constant frequency ratio $\tau = 5$, $K = 0.01$ upon varying rescaled plank's constant $\hbar_{eff}$. (b) for $\hbar_{eff} = 1$ when different kicking strength K are considered, at the same frequency ratio. The initial state was taken as a product of the ancilla and coherent state with $\alpha = 2$.

The results can be explained by explicitly writing the cosine hyperbolic part of the Floquet operator in terms of its summation series and noting the contributions of $\hbar_{eff}$ in the kick part. Eq. (5) then becomes

$$\hat{F} = e^{-i(\hat{a}^\dagger\hat{a}+\frac{1}{2})\tau} e^{i\left[\frac{K}{\hbar_{eff}}+\frac{K}{2!2!}(\hat{a}+\hat{a}^\dagger)^2+\frac{K}{2^2.4!}\hbar_{eff}(\hat{a}+\hat{a}^\dagger)^4+.....\right]|0_Z\rangle\langle 0_Z|}. \quad (17)$$

This signifies that entanglement is mostly influenced by the terms containing K and $\hbar_{eff}$ in the kicking part, with $e^{[i\frac{K}{\hbar_{eff}}]|0_Z\rangle\langle 0_Z|}$ only contributing a relative phase to the ancilla. To see this we have plotted entanglement versus number of kicks by varying K in Fig. 5 (below) for a constant $\hbar_{eff}$. The result implies that entanglement rise almost linearly for our previously chosen kicking strength, i.e. $K = 0.01$. Hence, it is a prime domain for testing the above relation's dependence upon $\hbar_{eff}$. Now, if $\hbar_{eff}$ is taken to be very small entanglement becomes entirely dependent on $e^{[i\frac{K}{2!2!}(\hat{a}+\hat{a}^\dagger)^2]|0_Z\rangle\langle 0_Z|}$, which is $\hbar_{eff}$ independent. Thus for a fixed value of K entanglement rate has the same curve, no matter how small we let $\hbar_{eff}$ be. The saturation rate vanishes for $K = 0.001$ even at $\hbar_{eff} = 1$, see Fig. 5(below). On the other hand, as the value of $\hbar_{eff}$ is increased the survival of higher order terms contribute to the sum and an increase in entanglement is observed. Same trends are being followed by other initial conditions, i.e. product of ancilla with fock state.

5 Conclusion

We study the entanglement dynamics of conditional kicked membrane in an optomechanical system. It is shown that the frequency ratio $\tau = \pi$ always optimize the entanglement no matter which ancilla state is taken as an initial condition. While rational multiples $\tau \epsilon p\pi$ enhances entanglement only for initial coherent state, no enhancement is seen for Fock state. Impulsive increase in entanglement with a delta pulse of large kicking strength is observed and mainly follows from the increased stochasticity for larger amplitude of the kick. Furthermore, it is reported that entanglement is enhanced by increasing $\hbar_{eff}$, while it drops for a decrease in the value of $\hbar_{eff}$, unless entanglement rate saturates. This is a remarkable outcome as it quantifies a transition to classical chaos. Moreover, the values of parameters considered in our simulations satisfy current experimental values used in the laboratory experiments. For future perspective, the state fidelity analysis of kicked membrane driven by varying kicking strength is a future endeavor to discern quantum-classical transitions of chaos.

6 References

1 S. Mancini, D. Vitali, V. Giovannetti and P. Tombesi, *Eur. Phys. J. D*, **22**, 41722 (2003).
2 M. Pinard, A. Dantan, D. Vitali, O. Arcizet, T. Briant and A. Heidmann, *Europhys. Lett.*, **72**, 747 (2005).
3 D. Vitali, S. Mancini and P. Tombesi, *J. Phys. A: Math. Theor.*, **40**, 805568 (2007).
4 S. Bose, K. Jacobs and P. L. Knight, *Phys. Rev. A*, **56**, 417586 (1997).
5 W. Marshall, C. Simon, R. Penrose and D. Bouwmeester, *Phys. Rev. Lett.*, **91**, 130401 (2003).
6 J. D. Teufel, T. Donner, D. Li, J. W. Harlow, M. S. Allman, K. Cicak, A. J. Sirois, J. D. Whittaker, K. W. Lehnert, and R. W. Simmonds, *Nature*, **475**, 359 (2011).
7 M. A. Nielsen and I. L. Chuang, *Quantum Computation and Quantum Information*, Cambridge University Press, Cambridge, U.K. (2000).

8 K. Furuya, M. C. Nemes, and G. Q. Pellegrino, *Phys. Rev. Lett.*, **80**, 5524 (1998).
9 J. N. Bandyopadhyay and A. Lakshminarayan, *Phys. Rev. Lett.*, **89**, 060402 (2002).
10 D. L. Shepelyansky, *Phys. Rev. A*, **67**, 054303 (2003).
11 P. Jacquod, *Phys. Rev. Lett.*, **92**, 150403 (2004).
12 T. M. Fromhold et al, *Phys. Rev. Lett.*, **87**, 046803 (2001).
13 S. Wimberger, R. Mannella, O. Morsch and E. Arimondo, *Phys. Rev. Lett.*, **94**, 130404 (2005).
14 S. A. Gardiner, J. I. Cirac and P. Zoller, *Phys. Rev. A*, **79**, 4790 (1997).
15 D. A. Steck, Phd Dissertation, Raizen Labs Texas University (2001).
16 B. Lemos Gabriela, R. M. Gomes, S. P. Walborn, P. H. S. Ribeiro and F. Toscano, *Nat. Commun.*, **3**, 1211 (2012).
17 X. G. Wang, S. Ghose, B. C. Sanders, and B. Hu, *Phys. Rev. E*, **70**, 016217 (2004).
18 H. Fujisaki, T. Miyadera, and A. Tanaka, *Phys. Rev. E*, **67**, 066201 (2003).
19 M. Aspelmeyer, T. J. Kippenberg, and F. Marquardt, *Rev. Mod. Phys.*, **86**, 1391 (2014)
20 C.-P. Sun, Y. Li, Science China Physics, *Mechanics and Astronomy*, **58**, 050300 (2015).
21 W. Ge, M.Al-Amri, H. Nha, and M. S. Zubairy, *Phys. Rev. A*, **88**, 022338 (2013).
22 E. A. Sete and H. Eleuch, *J. Opt. Soc. Am. B*, **32**, 971-982 (2015).
23 M. J. Hartmann, and M. B. Plenio, *Phys. Rev. lett.*, **101**, 200503 (2008).
24 L. Zhou, Y. Han, J. Jing, and W. Zhang, *Phys. Rev. A*, **83**, 052117 (2011).
25 H. Wang, X. Gu, Y.-x. Liu, A. Miranowicz, and F. Nori, *Phys. Rev. A*, **92**, 033806 (2015).
26 R.-X. Chen, L.-T. Shen, Z.-B. Yang, H.-Z. Wu, S.-B. Zheng, *Phys. Rev. A*, **89**, 023843 (2014).
27 M. Abdi, M. J Hartmann, *New J. Phys.*, **17**, 013056 (2015).
28 L. Tian, Phys. Rev. Lett., **110**, 233602 (2013).
29 M. J. Akram, F. Saif, *Nonlinear Dyn.*, **83**, 963-970 (2016).
30 Yong. Li, Lian-Ao Wu, and Z. D. Wang, *Phys. Rev. A*, **83**, 043804 (2011)
31 C. Galland, N. Sangouard, N. Piro, N. Gisin, and T. J. Kippenberg, *Phys. Rev. lett.*, **112**, 143602 (2014).
32 S. Hong, R. Riedinger, I. Marinković, A. Wallucks, S. G. Hofer, R. A. Norte, M. Aspelmeyer, and S. Gröblacher, *Science*, **358** 203 (2017).
33 M. M. Khan, M. J. Akram, F. Saif, *Phys. Rev. A*, **94**, 063830 (2016).
34 Eric G Arrais, J. S. Sales and N. G. de Almeida, *J. Phys. B: At. Mol. Opt. Phys.*, **49**, 165501 (2016).
35 T. Huan, R. Zhou, Hou. Ian, *Phys.Rev.A*, **92**, 022301 (2015).
36 M. G. A. Paris, *Phys. Rev. A*, **59**, 1615 (1999).
37 L. F. Quezada, E. Nahamad-Achar, *Entropy*, **20**, 72 (2018).
38 T. -C. Wei, K. Nemoto, P. M. Goldbart, P. G. Kwait, W. J. Munro and F. Verstraete, *Phys. Rev. A*, **67**, 022110 (2003).
39 K. Berrada, M. EI. Baz, F. Saif, Y. Hassouni and S. Mnia, *J. Phys. A: Math. Theor.*, **42**, (2009).
40 M. Engel, *On Quantum chaos, Stochastic Webs and Localization in a Quantum Mechanical Kick system*, Ph.D. dissertation (2003).